
An open-source framework for bioprinting quality optimisation

Pablo Martín Compaired¹, Elena García Garetá^{1,2,3}, María Ángeles Pérez^{1,2}

¹ Multiscale in Mechanical & Biological Engineering Research Group, Aragon Institute of Engineering Research (I3A), School of Engineering & Architecture, University of Zaragoza, 50018 Zaragoza, Aragon, Spain.

² Aragon Institute for Health Research (IIS Aragon), Miguel Servet University Hospital, 50009 Zaragoza, Aragon, Spain.

³ Division of Biomaterials & Tissue Engineering, UCL Eastman Dental Institute, University College London, London NW3 2PF, UK.

pablo.martin@unizar.es, garciae@unizar.es, angeles@unizar.es

Abstract

Bioprinting has emerged as a transformative technology in biomedical research, enabling the fabrication of highly customizable, cell-laden structures. However, widespread adoption remains limited due to challenges in achieving consistent, high-quality prints, because of to the absence of standardised protocols. In this study, we propose a systematic bioprinting approach to optimise the performance of an in house-made photo-curable biomaterial ink composed of gelatin methacryloyl (GelMA) and egg white proteins. Print quality is assessed based on three fundamental assays: extrusion consistency, deposition accuracy and overall printability. To enhance image-based analysis, we developed a custom 3D-printed lens mount for a USB-microscope, paired with a Python script for quantitative evaluation of bioprinting performance. Our results indicate a suitable printing pressure range combined with optimal printing speeds, identified as optimal for generating complex 3D structures. This study presents a robust methodology for evaluating and optimising key bioprinting parameters, such as pressure and speed, contributing to the development of standardised workflows to enhance reproducibility and facilitate the broader adoption of bioprinting in tissue engineering and regenerative medicine.

Bioprinting; Process standardisation; Custom image capturing; Photo-curable biomaterial ink; Gelatin methacryloyl (GelMA); Egg white proteins.

1. Introduction

Bioprinting, an advanced technology derived from additive manufacturing, has emerged as a key technique in tissue engineering [1]. This innovative approach enables the precise deposition of cells and biomaterials, facilitating the fabrication of complex biological structures [2]. Over the past decade, bioprinting has gained the interest in diverse biomedical fields, including regenerative medicine, drug testing, cancer research, and personalized medicine [3]. As the field evolves, numerous printing techniques have been developed, including droplet-based, laser-assisted, extrusion-based and stereolithography, each with distinct advantages and limitations depending on the target application [4]. Despite these advancements, the reproducibility and standardisation of bioprinting processes remains a major challenge. The increasing adoption of bioprinting has led to the proliferation of various printing techniques and bioink formulations, consequently diverse characterization methods have been proposed to assess bioprinting quality, yet there is not universally accepted standard [5]. Many of these approaches require specialized equipment or involve complex assays, which may introduce variability and limit the comparability of results across research groups [6,7].

A critical gap in the field lies in the need for an accessible, reproducible, and quantitative framework to evaluate bioprinting quality [8]. To address this issue, we propose a systematic methodology centred on three key parameters: extrudability, filament deposition and printability. These metrics cover essential aspects of the bioprinting process, from material

flow to structural fidelity and provide a comprehensive yet practical assessment of printing performance.

To facilitate this analysis, we have developed a suite of customized software and hardware tools. A dedicated application generates G-code tailored for bioprinting assays, ensuring consistency in experimental conditions. Following printing, high-resolution image acquisition is achieved using a USB-microscope mounted on a custom-designed 3D-printed support system, enabling fast data collection. A Python-based script then automates image quantification, streamlining the analysis and enhancing reproducibility. By integrating these elements, our approach aims to establish a standardised and efficient method for evaluating bioprinting quality, ultimately contributing to the advancement of the field.

2. Materials and Methods

2.1. Hydrogel solution

An in house-made hydrogel solution was formulated for cell and cancer research, consisting of 10% (w/v) GelMA, 2% (w/v) egg white, and 0.5% (w/v) LAP. This composition was designed to optimise biocompatibility, mechanical stability, and printability, making it suitable for bioprinting applications and three-dimensional cell culture.

Gelatin methacryloyl (GelMA), a chemically modified derivative of gelatin, provides an extracellular matrix mimicking environment, promoting cell adhesion, proliferation, and migration due to its intrinsic bioactive motifs [9]. Furthermore, its photocrosslinking capability enables tuneable mechanical properties through controlled UV exposure, ensuring the structural integrity of bioprinting constructs [10].

Lithium phenyl-2, 4, 6-trimethylbenzoylphosphine (LAP) serves as a photoinitiator, enabling rapid photocrosslinking

under visible light (405 nm). It was selected for its high reactivity at low concentrations, enabling fast polymerization with minimal cytotoxicity. Compared to traditional UV-based photoinitiators, LAP reduces the generation of free radicals, thereby enhancing cell viability [11].

The incorporation of egg white further enhances the hydrogel's biological functionality. Rich in bioactive proteins and growth factors, egg white has been shown to support angiogenesis and cell proliferation, making it particularly relevant for tumor microenvironment modelling and tissue regeneration [12]. Its inclusion aims to improve the hydrogel's suitability for advanced 3D tissue models, providing a physiologically relevant platform for investigating cancer progression and evaluating therapeutic strategies [13].

This biomaterial ink exhibits non-Newtonian shear-thinning behaviour with a characteristic yield stress, making it well-suited for extrusion-based bioprinting techniques. Its photocrosslinking capability ensures structural integrity post-printing, while its rich protein content enhances cellular activity, promoting cell adhesion, proliferation, and functionality within the printed construct.

2.2. Bioprinting quality assays

The evaluation of bioprinting quality is conducted through the proposed framework, which comprises three distinct tests.

The first test, extrudability, identifies the optimal printing pressure values for consistent extrusion by setting a range of pressures (0-100 KPa) and analysing the weight of the deposited solution. This step is essential to determine the minimum printing pressure required to overcome the yield stress of the biomaterial ink, ensuring it transitions from a static to a flowing state. By identifying this threshold, the test helps establish the lowest pressure at which the solution begins to extrude smoothly, preventing issues such as under-extrusion at lower pressures or over-extrusion at higher pressures [14].

Once optimal pressures are determined, the second test focuses on filament diameter optimisation, adjusting printing pressure and printing speed to match the printed filament diameter with the nozzle dimensions. This test is conducted to evaluate the fidelity of the extruded samples by comparing the actual filament diameter to the nozzle outlet diameter. By systematically varying the printing parameters – pressure and speed – the test ensures that the extruded filament maintains dimensional accuracy, minimizing deviations that could impact the structural integrity and resolution of the printed construct.

Finally, to evaluate 3D multilayer structural fidelity, a multilayer mesh structure is printed with the optimal printing parameters obtained previously, and the internal pore structure is analysed to evaluate the ability to form stable layers. This test ensures that the printed structure maintains its intended geometry across multiple layers, which is crucial for large scale applications, such as tissue scaffolds. By assessing pore uniformity of this mesh geometry, the test helps identify potential issues like filament dragging, layer collapse, or material spreading, which could compromise the overall 3D structural integrity and functionality of the construct.

To conduct the bioprinting assays, BIO X (Cellink, Gothenburg, Sweden) bioprinter was employed with a temperature-controlled printhead. After printing the samples, they were photo-crosslinked using a 405 nm UV lamp, ensuring that the samples reached the gelation state achieving the structural integrity post-printing.

2.3. Image analysis

Conventional microscopy is primarily designed for micro-scale imaging. While some techniques allow for the reconstruction of larger-scale images, they are often time-consuming and resource-intensive, making them less efficient for capturing bioprinted structure at the macro scale. To address these limitations, a USB-microscope is employed for imaging the bioprinted constructs, providing a faster and more accessible alternative to conventional microscopy. The USB-microscope, capable of magnification up to 4K resolution, is mounted on a custom 3D-printed support equipped with three-axis control (Figure 1), integrating stepper motors for precise focusing adjustment. This setup ensures reproducible imaging conditions and minimises human error when analysing multiple samples.

Furthermore, the system includes integrated LED illumination with custom light diffusion filters to enhance image clarity and consistency, reducing shadows and optical artifacts that may interfere with image analysis. Compared to the conventional stitched microscopy, this approach enables rapid acquisition of macro-scale images with minimal setup time, facilitating efficient and standardised bioprinting quality assessments. Moreover, by utilizing a cost-effective USB-microscope instead of high-end imaging systems, this method reduces financial barrier to bioprinting analysis, promoting the democratization of image capture in both research and industrial fields.

Finally, to streamline image analysis and quantification, a custom Python script was developed to assess filament deposition test by measuring filament width using the 2D local thickness principle and assess printability test obtained pores through a border-following algorithm.

For filament width measurement, the process involves image sampling, cropping, and converting the filament image to a binary mask. A distance transform calculates the Euclidean distance from each point to the nearest boundary, providing an estimate of the filament diameter. A thresholding step removes small, irrelevant regions, followed by a dilation operation to refine thickness values. The final local thickness is determined by identifying the largest possible inscribed circle within the filament, ensuring precise diameter evaluation through all the constructs. For pore analysis, the multilayer structure image is cropped and binarised to isolate pores. The pore surface area is computed by summing all the pixels in the pore mask, while a border-following algorithm detects contours for perimeter estimation [15]. The Euclidean distance between successive contour points is summed to obtain the total perimeter, allowing for accurate pore measurement and printability assessment.

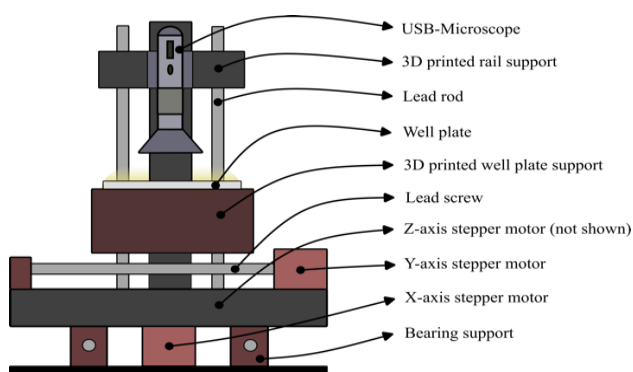


Figure 1. USB-microscope lens support designed for image capturing the bioprinted samples.

3. Results and Discussion

The proposed working framework begins with the extrudability test, identifying 65 KPa as the minimum pressure

required to overcome the hydrogel's yield stress and initiate extrusion. Below that printing pressure value, no solution was extruded through the nozzle. Within the 70-80 KPa range, mass flow rate increases steadily with good deposition consistency, making it the optimal printing pressure condition. In contrast, pressures exceeding 85 KPa introduce significant variability, leading to over-extrusion and compromising print quality (Analysis not shown). These findings align with the previous studies on extrusion bioprinting, which indicate that increasing printing pressure improves flow deposition rate but also enhances potential instability at higher values [16,17].

The second assessment, deposition test, further reinforced the previous observations, demonstrating that increased printing pressure or reduced printing speed resulted in greater deposition, whereas lower pressure and higher speed led to insufficient deposition (Figure 2). The results identified three optimal parameter combinations: 70 KPa at 300 mm/min, 75 KPa at 600 mm/min, and 80 KPa at 900 mm/min. Among these, the combination of 70 KPa and 300 mm/min yielded the most accurate surface and diameter values relative to theoretical filament model, exhibiting better consistency and reduced variability (Figure 2). This outcome suggests that at 70 KPa and 300 mm/min, the interplay between extrusion rate and material deposition is well-balanced, leading to a uniform and defined filament geometry. In contrast, the higher-pressure settings (75 KPa and 80 KPa) induced greater material deposition, but this came at the cost of increased filament variability, as reflected in the larger standard deviations (Figure 2). Additionally, an important factor to consider is the material behaviour under dynamic printing conditions. At higher speeds, the material deposition per unit length is reduced, which explains why the filaments printed at 900 mm/min, despite being extruded at higher printing pressure values (80 KPa), exhibited an overall smaller surface area compared than those printed at lower speeds. This indicates that the deposition rate is not solely a function of printing pressure but is also significantly modulated by speed. Overall, these findings align with existing research on extrusion-based bioprinting deposition dynamics, which emphasizes that interplay between pressure and speed [18,19].

Finally, the printability test was conducted to assess these optimised printing conditions, identifying 75 KPa at 600 mm/min as the most favourable combination. Although all tested printing conditions produced well-defined pores matching theoretical values, both lower (70 KPa at 300 mm/min) and higher (80 KPa at 900 mm/min) settings introduced significant variability (Analysis not shown). The high statistical significance ($p < 0.001$) observed between intermediate and high printing conditions suggest that increased speed and pressure may compromise structural stability (Analysis not shown). These findings emphasize the need for comprehensive evaluations beyond previous filament deposition, as early tests alone suggested 70 KPa at 300 mm/min as optimal. Instead, further analysis demonstrated that 75 KPa at 600 mm/min resulted in more consistent constructs, highlighting the critical role of structural integrity and deposition precision in bioprinting quality. These observations align with previous studies on 3D complex printing analysis, where fine-tuning printing parameters is required to optimise the final constructs [20,21].

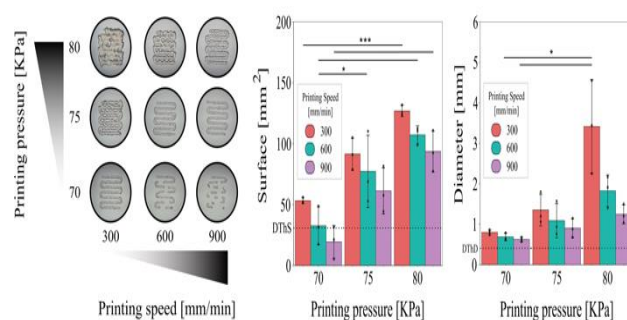


Figure 2. Deposition test results at different printing conditions. Being DTs and DTd the theoretical surface and diameter values of the filament respectively. All statistical tests were conducted at a significance level of $\alpha = 0.05$. The results presented as the mean standard deviation. Statistical significance was indicated using the following notation: “*” ($p < 0.05$), “**” ($p < 0.01$) and “***” ($p < 0.001$).

4. Summary

This study presents a systematic framework for optimising bioprinting through extrudability, deposition and printability tests. The proposed biomaterial ink exhibits a shear-thinning, non-Newtonian behaviour with a yield stress related to a printing pressure of 65 KPa (Image not shown). Printing pressure significantly influenced extrusion flow, with an optimal range identified between 70-80 KPa (Image not shown). A detailed analysis revealed that high-quality filament deposition was achieved at 70 KPa with 300 mm/min, 75 KPa with 600 mm/min, and 80 KPa with 900 mm/min (Figure 2). Among these, 75 KPa and 600 mm/min provided the best balance between extrusion consistency and 3D shape fidelity (Image not shown), making it the most suitable condition for fabricating complex constructs.

Furthermore, this study integrates an accessible and cost-effective imaging solution using a USB-microscope mounted on a custom 3D-printed lens support, enabling reproducible and high-resolution image acquisition for bioprinting quality analysis. Additionally, a Python-based image processing script automates bioprinting test analysis quantification, streamlining the assessment process while minimizing human error. By combining these tools, this framework significantly reduces dependence on expensive imaging equipment and complex manual analyses, enhancing reproducibility and accessibility.

5. Conclusion

The proposed framework characterises 3D bioprinting process quality assessment with three essential assays and provide a method for determining appropriate printing parameters to enable optimization studies. The system includes the integration of a USB-microscope with a custom 3D-printed lens support and an automated Python-based analysis pipeline democratizes quality assessment, making it a readily accessible solution. This approach helps enable reproducible and scalable 3D bioprinting that can be adopted across different laboratories and industrial fields, thereby helping to develop standards in the industry.

6. Future work

Given the non-Newtonian behaviour of bioinks and the significant impact of shear stress on cell viability in extrusion-based bioprinting, further investigation is required. CFD simulations can play a fundamental role for understanding this phenomenon. Therefore, further investigations will involve multiple simulations under varying printing conditions to enhance cell viability and drive advancements in 3D bioprinting.

However, this study presents certain limitations. The imaging approach used is only suitable for top-view analysis, which restricts the ability to assess filament geometry and structural integrity in three dimensions. Additionally, nozzle type plays a crucial role in extrusion mechanics, influencing flow behaviour and deposition accuracy. Future studies will incorporate a detailed nozzle analysis to evaluate its impact on bioprinting quality, considering factors such as geometry and diameter properties.

By addressing these limitations, the proposed framework can be further refined to enhance its applicability and reliability in diverse bioprinting scenarios.

7. Acknowledgements

This work has been supported by the Spanish Government by “Plan de Recuperación Transformación y Resiliencia” and by the Europe Union “NextGenerationEU” (Progama Investigo 076-16). E.G.G is funded by a Ramón & Cajal Fellowship (RYC2021-033490-I), funded by MCIN/AE/10.13039/501100011033 and the EU” NextGenerationEU/PRTR”. Additional support has been received by Spanish Ministry of Science and Innovation through the Grants No PID2020-113819RB-I00 and PID2023-146072OB-I00.

References

- [1] Matai I, Kaur G, Seyedsalehi A, McClinton A and Laurencin C T 2020 Progress in 3D bioprinting technology for tissue/organ regenerative engineering *Biomaterials* **226**
- [2] Xu H, Liu J, Zhang Z and Xu C 2022 Cell sedimentation during 3D bioprinting: a mini review *Bioaddit Manuf* **5** 617–26
- [3] Vanaei S, Parizi M S, Vanaei S, Saleemizadehparizi F and Vanaei H R 2021 An Overview on Materials and Techniques in 3D Bioprinting Toward Biomedical Application *Engineered Regeneration* **2** 1–18
- [4] Wu C A, Zhu Y and Woo Y J 2023 Advances in 3D Bioprinting: Techniques, Applications, and Future Directions for Cardiac Tissue Engineering *Bioengineering* **10**
- [5] Strauß S, Grijalva Garces D and Hubbuch J 2023 Analytics in Extrusion-Based Bioprinting: Standardized Methods Improving Quantification and Comparability of the Performance of Bioinks *Polymers (Basel)* **15**
- [6] Rodríguez-Rego J M, Mendoza-Cerezo L, Macías-García A, Carrasco-Amador J P and Marcos-Romero A C 2022 Methodology for characterizing the printability of hydrogels *Int J Bioprint* **9** 280–91
- [7] Xu J, Yang S, Su Y, Hu X, Xi Y, Cheng Y Y, Kang Y, Nie Y, Pan B and Song K 2023 A 3D bioprinted tumor model fabricated with gelatin/sodium alginate/decellularized extracellular matrix bioink *Int J Bioprint* **9** 109–30
- [8] Fu Z, Naghieh S, Xu C, Wang C, Sun W and Chen X 2021 Printability in extrusion bioprinting *Biofabrication* **13**
- [9] Yue K, Trujillo-de Santiago G, Alvarez M M, Tamayol A, Annabi N and Khademhosseini A 2015 Synthesis, properties, and biomedical applications of gelatin methacryloyl (GelMA) hydrogels *Biomaterials* **73** 254–71
- [10] Gaglio C G, Baruffaldi D, Pirri C F, Napione L and Frascella F 2024 GelMA synthesis and sources comparison for 3D multimaterial bioprinting *Front Bioeng Biotechnol* **12**
- [11] Elkhoury K, Zuazola J and Vijayavenkataraman S 2023 Bioprinting the future using light: A review on photocrosslinking reactions, photoreactive groups, and photoinitiators *SLAS Technol* **28** 142–51
- [12] Jalili-Firoozinezhad S, Filippi M, Mohabatpour F, Letourneur D and Scherberich A 2020 Chicken egg white: Hatching of a new old biomaterial *Materials Today* **40** 193–214
- [13] Pele K G, Amaveda H, Mora M, Marcuello C, Lostao A, Alamán-Díez P, Pérez-Huertas S, Ángeles Pérez M, García-Aznar J M and García-Gareta E 2023 Hydrocolloids of Egg White and Gelatin as a Platform for Hydrogel-Based Tissue Engineering *Gels* **9**
- [14] Gao T, Gillispie G J, Copus J S, Kumar A P R, Seol Y J, Atala A, Yoo J J and Lee S J 2018 Optimization of gelatin-alginate composite bioink printability using rheological parameters: A systematic approach *Biofabrication* **10**
- [15] Suzuki S 1985 *Topological Structural Analysis of Digitized Binary Images by Border Following*
- [16] Paxton N, Smolan W, Böck T, Melchels F, Groll J and Jungst T 2017 Proposal to assess printability of bioinks for extrusion-based bioprinting and evaluation of rheological properties governing bioprintability *Biofabrication* **9**
- [17] O’Connell C, Ren J, Pope L, Li Y, Mohandas A, Blanchard R, Duchi S and Onofrillo C 2020 Characterizing Bioinks for Extrusion Bioprinting: Printability and Rheology *Methods in Molecular Biology* vol 2140 (Humana Press Inc.) pp 111–33
- [18] Zhou K, Dey M, Ayan B, Zhang Z, Ozbolat V, Kim M H, Khristov V and Ozbolat I T 2021 Fabrication of PDMS microfluidic devices using nanoclay-reinforced Pluronic F-127 as a sacrificial ink *Biomedical Materials (Bristol)* **16**
- [19] Webb B and Doyle B J 2017 Parameter optimization for 3D bioprinting of hydrogels *Bioprinting* **8** 8–12
- [20] Daly A C, Critchley S E, Rencsok E M and Kelly D J 2016 A comparison of different bioinks for 3D bioprinting of fibrocartilage and hyaline cartilage *Biofabrication* **8**
- [21] Freeman F E and Kelly D J 2017 Tuning alginate bioink stiffness and composition for controlled growth factor delivery and to spatially direct MSC Fate within bioprinted tissues *Sci Rep* **7**